Title	Effect of transforming growth factor-β1 on functional expression of monocarboxylate transporter 1 in alveolar epithelial A549 cells
Author(s)	Uddin, Mohi; Kawami, Masashi; Yumoto, Ryoko; Takano, Mikihisa
Citation	Naunyn-Schmiedeberg's Archives of Pharmacology , 393 (5) : 889 - 896
Issue Date	2020-05
DOI	10.1007/s00210-019-01802-3
Self DOI	
URL	https://ir.lib.hiroshima-u.ac.jp/00050464
Right	This is a post-peer-review, pre-copyedit version of an article published in Naunyn-Schmiedeberg's Archives of Pharmacology. The final authenticated version is available online at: https://doi.org/10.1007/s00210-019-01802-3 This is not the published version. Please cite only the published version. この論文は出版社版ではありません。引用の際には出版社版をご確認、ご利用ください。
Relation	

Naunyn-Schmiedeberg's Archives of Pharmacology
Original Article

1. Title page

Effect of transforming growth factor-β1 on functional expression of monocarboxylate transporter 1 in alveolar epithelial A549 cells

Mohi Uddin, Masashi Kawami, Ryoko Yumoto, Mikihisa Takano

Department of Pharmaceutics and Therapeutics, Graduate School of Biomedical and Health Sciences, Hiroshima University, 1-2-3 Kasumi, Minami-ku, Hiroshima 734-8553, Japan

To whom correspondence should be addressed: Mikihisa Takano, Department of Pharmaceutics and Therapeutics, Graduate School of Biomedical and Health Sciences, Hiroshima University, 1-2-3 Kasumi, Minami-ku, Hiroshima 734-8553, Japan
Telephone number: +81-82-257-5315; FAX number: +81-82-257-5319
E-mail address: takanom@hiroshima-u.ac.jp

Acknowledgements

This work was supported in part by a Grant-in-Aid for Scientific Research from the Japan Society for the Promotion of Sciences (JSPS) (numbers; 26293033, 15K08074, and 16K18945).

ORCID IDs

Kawami-M; 0000-0003-2162-6769
Takano-M; 0000-0003-2865-3129

2. Abstract

Epithelial-mesenchymal transition (EMT) contributes to the development of severe lung diseases, such as pulmonary fibrosis. Recently, it has been reported that EMT involves complex metabolic reprogramming triggered by several factors including transforming growth factor (TGF-β1) and that monocarboxylate transporter (MCT1) plays an essential role in these metabolic changes. The aim of the present study was to clarify the functional expression of MCT1 during TGF-β1-induced EMT in alveolar epithelial A549 cells. The transport function of MCT1 in A549 cells was examined using [^{3}H]γ-hydroxybutyrate (GHB) and [^{3}H]lactic acid (LA) as substrates and α-cyano-4-hydroxycinnamate (CHC), lactic acid, phloretin, and AR-C155858 (AR) as inhibitors of MCT1. EMT was induced by treating the cells with TGF-β1. mRNA and protein expression levels were analyzed using real-time PCR and western blotting, respectively. Time-, temperature-, and pH-dependent GHB and LA uptake were observed in A549 cells. CHC, lactic acid, phloretin, and AR significantly inhibited the uptake of GHB in a concentration-dependent manner, suggesting that MCT1 is primarily responsible for transport of monocarboxylates such as GHB and LA in A549 cells. TGF-β1 treatment significantly enhanced GHB and LA uptake as well as the mRNA and protein expression levels of MCT1 in A549 cells. These changes were neutralized by co-treatment with SB431542, an inhibitor for the TGF-β1 signaling pathway. CHC and AR had no effect on TGF-β1-induced EMT-related gene expression changes. Here, we have clearly characterized functional expression of MCT1 in A549 cells and have shown that MCT1 may be upregulated via the TGF-β1 signaling pathway.

3. Keywords

alveolar epithelial cells; epithelial-mesenchymal transition; γ-hydroxybutyrate; monocarboxylate transporter 1; transforming growth factor-β1

4. Abbreviations

CK19, cytokeratin 19; EMT, epithelial-mesenchymal transition; GHB, γ-hydroxybutyrate; SB, SB431542; α-SMA, α-smooth muscle actin; TGF-β1, transforming growth factor-β1; GAPDH, glyceraldehyde-3-phosphate dehydrogenase

5. Introduction

Pulmonary fibrosis is a chronic respiratory disease in which the lung tissues become scarred, thickened, and stiff, resulting in reduced oxygen supply to the blood. Therefore, patients develop perpetual shortness of breath. In most cases, the definite cause and underlying mechanism of the disease remain unclear. However, it is now recognized that epithelial-mesenchymal transition (EMT) plays an essential role in the development of pulmonary fibrosis and that transforming growth factor (TGF)-β1 can induce EMT by activating important signaling pathways (Kalluri and Neilson 2003; Willis and Borok 2007; Kalluri and Weinberg 2009). In alveolar epithelial A549 cells, TGF-β1 induces EMT-like phenotypical changes via the TGF-β signaling pathway that involves SMAD2 activation (Takano et al. 2015; Kawami et al. 2016). Although there is no effective approach for the prevention of pulmonary fibrosis, several types of inhibitors against TGF-β1 are considered candidates for EMT suppressor agents (Connolly et al. 2012).

Recently, it has been reported that the EMT is associated with complex metabolic reprogramming (Kang et al. 2019). In tumor cells, metabolic adaptations lead to an increase in glucose uptake and lactate secretion, thereby contributing to an acidic microenvironment, which is followed by the induction of EMT (Liu et al. 2016; Morandi et al. 2017). Lactate is transported across the plasma membrane by four proton-linked monocarboxylate transporters, MCT1–MCT4, belonging to the solute carrier *SLC16A* family (Fishbein et al. 2002; Halestrap and Meredith 2004; Halestrap and Wilson 2012). Among them, MCT1 is by far the best characterized isoform, and it is involved in the bidirectional transport of monocarboxylates such as lactate, indicating that MCT1 could play an essential role in

metabolic reprograming via regulation of the lactate shuttle. However, information concerning MCT1 activity in alveolar epithelial cells is limited, and the contribution of MCT1 to EMT has not been well-investigated.

MCT1 also plays a central role in tumor cell energy homeostasis. Therefore, the clinical development of MCT1 inhibitors for cancer therapy is on-going, and at least one MCT1 inhibitor, AZD3965, is currently under clinical trial (Guan et al. 2018, 2019). Thus, MCT1 is recognized as a novel target for cancer treatment. If the association of MCT1 with EMT is proven, MCT1 inhibition may be used to prevent EMT-related diseases, such as pulmonary fibrosis.

So far, A549 cells have been considered a suitable model for EMT studies (Kawami et al. 2016, 2018a), and it has been clarified that TGF-β1 induces EMT via upregulation of its signaling pathway. A previous report has also demonstrated the expression of MCT1 in A549 cells (Eilertsen et al. 2014). Considering these findings, A549 cells should be a good model for investigating the effect of TGF-β1 on the functional expression of MCT1. Therefore, the aims of the present study were to characterize MCT1 function and to examine the changes in expression and function of MCT1 during TGF-β1-induced EMT using A549 cells.

6. Materials and methods

Materials

Fetal bovine serum (FBS) and Dulbecco's modified Eagle's medium (DMEM) were purchased from MP Biomedicals (Solon, OH, USA). Trypsin-ethylenediaminetetraacetic acid (EDTA) and penicillin-streptomycin were purchased from Thermo Fisher Scientific Inc. (Waltham, MA, USA). TGF-β1 was purchased from BioLegend, Inc (San Diego, CA, USA). SB431542 was purchased from Wako Pure Chemicals Ind. (Osaka, Japan). [^{3}H] γ - hydroxybutyric acid (GHB) and [^{3}H]lactic acid (LA) were purchased from American radiolabeled chemicals, Inc. (St. Louis, MO, USA). All the other chemicals used for the experiments were of the highest purity that was commercially available.

Cell culture

A549 cells obtained from RIKEN BioResource Research Center (Tokyo, Japan) were cultured in DMEM containing 100 IU/mL penicillin, 100 µg/mL streptomycin, and 10% FBS in 5% CO_2 at 37 °C and were sub-cultured every seven days (after cell treatment with 1 mM EDTA and 0.25% trypsin) as described previously (Kawami et al. 2016). The medium was replaced every two or three days.

Uptake studies

A549 cells grown on a 24-well plate for six days were used for uptake studies. After removing the culture medium, the cells were washed twice with HEPES-buffered saline (HBS; 5 mM HEPES, 145 mM NaCl, 3 mM KCl, 1 mM $CaCl_2$, 0.5 mM $MgCl_2$, and 5 mM glucose, pH 7.4) and preincubated with HBS at 37 °C for 10 min. Then, the cells were incubated with HBS or MES-buffered saline (MBS; 5 mM MES, 145 mM NaCl, 3 mM

KCl, 1 mM $CaCl_2$, 0.5 mM $MgCl_2$, and 5 mM glucose, pH 6) containing 100 nM GHB at 37 °C or 4 °C for 0.25–5 min. For inhibition studies, the cells were incubated with [^{3}H] GHB or [^{3}H]LA at 37 °C for 1 min in the absence or presence of various concentrations of CHC (0.5, 1, 2 mM), phloretin (10, 20, 100 µM), non-labeled LA (1, 5, 10 mM), and AR-C155858 (AR) (1, 3, 10, 30, 60, 100, 1000 nM) in HBS or MBS. After the incubation, the uptake buffer was aspirated, and the cells were rinsed with ice-cold phosphate-buffered saline (PBS; 137 mM NaCl, 3 mM KCl, 8 mM Na_2HPO_4, 1.5 mM KH_2PO_4, 0.1 mM $CaCl_2$, and 0.5 mM $MgCl_2$, pH 7.4). The cells were scraped and solubilized with NaOH for 30 min at approximately 22°C, and then centrifuged at 9838×*g* for 5 min. The supernatant was then used for either radioactivity counting or protein assay. For the measurement of [^{3}H]GHB or [^{3}H]LA uptake, 3 mL of Ultima GOLD (PerkinElmer, MA, USA) was added, and the radioactivity was measured by liquid scintillation counting on a LSC5100 (Hitachi Aloka Medical Ltd., Tokyo, Japan). Protein concentration was measured by the Bradford method using bovine serum albumin as a standard.

Calculation of the Ki value of CHC to MCT1 using a Dixon plot was achieved by linear regression analysis of reciprocal saturable uptake (1/v) for different GHB or LA concentrations (25 or 50 nM) as a function of CHC inhibition concentrations.

Real-time PCR

Total RNA was extracted from the cells and reverse transcribed into cDNA using ReverTra Ace (Toyobo, Osaka, Japan). Real-time PCR was performed on a Bio-Rad CFX96 (Bio Rad, Hercules, CA, USA) using KAPA SYBR® FAST qPCR Kit, as described previously (Kawami et al. 2018a). The PCR conditions were as follows: initial denaturation for 1 cycle

of 30 s at 95 °C, followed by specified number of cycles of 5 s at 95 °C (denaturation), 20 s at 60 °C (annealing), and 15 s at 72 °C (extension). The primer sequences for MCT1 were as follows: 5′-TGGCTGTCATGTATGGTGGA -3′ (sense) and 5′-AAGTTGAAGGCAAGCCCAAG-3′ (antisense). The primers for cytokeratin 19 (CK19), alpha smooth muscle actin (α-SMA), and glyceraldehyde 3-phosphate dehydrogenase (GAPDH), were as reported previously [5]. The mRNA expression level of MCT1 was normalized to that of GAPDH, a housekeeping gene.

Western blotting

MCT1 protein in A549 cells was analyzed using the crude membrane fraction of the treated cells as described previously (Kawami et al. 2018b). The expression of MCT1 was examined using rabbit polyclonal anti-MCT1 antibodies (PA5-12335; 1:250 dilution) and HRP-linked donkey anti-rabbit IgG secondary antibodies (NA934; 1:5000 dilution). In these studies, GAPDH was used as a loading control. GAPDH was detected with rabbit polyclonal anti-GAPDH antibodies (G9545; 1:5000 dilution) using a luminescent image analyzer, LAS 4000 plus (GE Healthcare Japan Corporation, Tokyo, Japan).

Statistical analysis

Data were expressed as means ± S.E.M. Statistical analysis was performed by student's t-test or one-way ANOVA followed by Tukey's test for multiple comparisons. The level of significance was set at * $p < 0.05$ or ** $p < 0.01$.

7. Results

Characterization of MCT1 function in A549 cells

Firstly, we attempted to determine general characteristics of GHB and LA uptake in A549 cells. A linear time-dependent increase up to 1 min in [^{3}H]GHB and [^{3}H]LA uptake was observed in A549 cells. Compared to the uptake of both substrates at 37 °C, the uptake of both substrates was markedly suppressed at 4 °C (Fig. 1a). As MCT1 is known to be a proton-coupled symporter, the effect of extracellular pH on GHB and LA uptake was examined. As expected, [^{3}H]GHB and [^{3}H]LA uptake at pH 6.0 was much higher than that at pH 7.4 (Fig. 1b).

There are several different inhibitors of MCT1, including the non-selective inhibitors such as α-cyano-4-hydroxycinnamate (CHC), LA, and phloretin, and the selective inhibitor AR. The effects of these inhibitors on GHB and LA uptake were examined. The Dixon plot revealed that concentration-dependent inhibition of [^{3}H]GHB and [^{3}H]LA uptake by CHC was competitive inhibition with Ki values of 0.84 and 1.75 mM, respectively (Fig. 2a). These values were comparable to the previously reported Ki value for CHC to MCT1 (Bröer et al. 1999). In addition, both LA and phloretin significantly suppressed [^{3}H]GHB uptake in a concentration-dependent manner (Figs. 2b, c). Furthermore, AR suppressed the uptake of both substrates in a concentration-dependent manner (Fig. 2d). These findings indicate that MCT1 is a functioning monocarboxylate transporter in A549 cells.

Role of the TGF-β signaling pathway in functional expression of MCT1 in A549 cells

We confirmed that 10 ng/mL of TGF-β1 treatment for 72 h markedly induced EMT-like phenotypical changes in A549 cells (Kawami et al. 2016). During TGF-β1-induced EMT,

however, it was unclear whether functional expression of MCT1 changes or not. Therefore, the effect of TGF-β1 on uptake of GHB and LA as well as mRNA and protein expression levels of MCT1 was examined. The role of the TGF-β signaling pathway in TGF-β1-induced alteration of MCT1 was also examined using SB431542 (SB), a TGF-β type I receptor kinase inhibitor. TGF-β1 significantly enhanced the uptake of [^{3}H]GHB and [^{3}H]LA in A549 cells, and these changes were neutralized by co-treatment with SB. (Fig. 3a). In addition, TGF-β1 treatment led to an enhancement of mRNA and protein expression levels of MCT1, and co-treatment with SB suppressed the upregulation of MCT1 induced by TGF-β1 (Figs. 3b, c). These findings suggest that the TGF-β signaling pathway may be closely associated with functional expression of MCT1 in A549 cells.

Contribution of MCT1 to TGF-β1-induced EMT in A549 cells

As CHC and AR inhibited the uptake of GHB and LA, we investigated the effect of these inhibitors on TGF-β1-induced EMT in A549 cells. At first, we examined the effects of CHC and AR on the morphological changes induced by TGF-β1. Both inhibitors had no effect on the morphological changes induced by TGF-β1 (Fig. 4a). In addition, known TGF-β1-induced alterations of mRNA expression such as a decrease in CK19 and an increase in α-SMA were not changed by co-treatment with CHC and AR (Fig. 4b, c). These findings suggest that TGF-β1-induced EMT may be independent of MCT1 function.

8. Discussion

Currently, idiopathic pulmonary fibrosis (IPF) represents one of the most severe respiratory diseases. A better understanding of the pathogenetic mechanisms of IPF would promote the development of new therapeutic strategies for this disease. However, the etiopathogenesis of and therapeutic interventions for IPF is not well-elucidated. Recently, EMT has been recognized as an important contributor to pulmonary fibrosis. In addition, several recent studies have reported an association between MCT1 and EMT (Liu et al. 2016; Morandi et al. 2017). In this study, therefore, we have focused on the link between MCT1 function and TGF-β1-induced EMT in A549 cells.

In the present study, we first attempted to characterize MCT1 function in A549 cells. In addition to the time-, temperature-, and pH-dependence of GHB and LA uptake in A549 cells, the inhibitory effects of several MCT1 inhibitors were observed. CHC is widely used as a MCT1 inhibitor, and the Ki value of CHC was previously shown to be 0.43 mM in oocytes expressing MCT1 (Bröer et al. 1999). This was comparable to the values obtained in this study (0.84 mM for GHB uptake and 1.75 mM for LA uptake). To our knowledge, this is the first study that has characterized the function of MCT1 in A549 cells. A549 cells, which are derived from human lung carcinoma, are a useful *in vitro* model of alveolar type II epithelial (ATII) cells (Lieber et al. 1976). ATII cells have a highly oxidative metabolic phenotype and are heavily dependent on mitochondrial function for energy production (Lottes et al. 2014). It has also been reported that these cells import lactate through MCT1 and use it as a substrate for mitochondrial energy production (Lottes et al. 2015). Our

findings regarding MCT1 function in A549 cells are consistent with the notion of mitochondrial metabolism as alternative fuel in ATII cells.

Kottman et al. (2012) reported the increased levels of lactate in the lung tissue of IPF patients. In addition, lactate derived from fibroblast foci can be used for ATP production via oxidative phosphorylation. MCT1 also plays an important role in the uptake of lactate in myofibroblasts (Tuder et al. 2012). To date, the regulation of MCT1 expression remains poorly understood. Although hypoxia inducible factor-1α is reported to be involved in the regulation of MCT4, there is no indication this factor is involved in MCT1 expression (Ullah et al. 2006). In the present study, we found that TGF-β1 induced GHB and LA uptake as well as the upregulation of mRNA and protein expression levels of MCT1 in A549 cells and that these effects were cancelled by co-treatment with SB. Therefore, the TGF-β signaling pathway may be involved in the regulation of the functional expression of MCT1.

The detailed mechanisms underlying regulation of MCT1 by TGF-β1 remain unclear at this moment. However, c-myc, an oncoprotein, is reported to directly control the transcription of MCT1 (Doherty et al. 2015). Therefore, the role of the TGF-β signaling pathway in mRNA expression of c-myc was examined. As shown in Supplementary Fig. 1, TGF-β1 significantly upregulated mRNA expression levels of c-myc. Additionally, SB suppressed TGF-β1-induced enhancement of c-myc mRNA expression. Thus, it is possible that c-myc may be associated with the regulation of MCT1 by TGF-β1 in A549 cells.

Among the members of *SLC16A* family, isoforms of MCT1-4 are known to be involved in monocarboxylate transport. MCT2 is expressed in restricted tissues, such as the liver

parenchyma and proximal convoluted tubule of the kidney (Payen et al. 2019). Likewise, MCT3, which exports lactate, is expressed only in retinal pigment epithelium and choroid plexus epithelium (Pinheiro et al. 2012). As shown in Supplementary Fig. 2, the mRNA expression level of MCT4 was not affected by TGF-β1 or by co-treatment with SB, indicating that MCT1 is the predominant isoform of MCTs affected by the TGF-β signaling pathway in A549 cells.

Our previous reports demonstrated that the RLE/Abca3 cell line derived from rat normal alveolar epithelium is a useful model to evaluate EMT (Takano et al. 2015, Kawami et al. 2017). Therefore, we attempted to examine the role of the TGF-β signaling pathway in functional expression of MCT1 using RLE/Abca3 cells. However, unfortunately, MCT1 activity was much lower in RLE/Abca3 cells than in A549 cells (data not shown), and it was difficult to evaluate the effect of TGF-β1 on the functional expression of MCT1 using this cell line. Further investigations using other alveolar epithelial cell lines with significant MCT1 activity should provide a better understanding of the relationship between EMT and functional expression of MCT1.

It has been reported that Warburg-like metabolic reprogramming in alveolar epithelial cells derived from IPF patients would result in increased glucose uptake mediated by glucose transporter 1 (GLUT1), a facilitative glucose transporter (Zank et al. 2018). Another report showed that aerobic glycolysis was enhanced during myofibroblast differentiation and lung fibrosis (Xie et al. 2015). Therefore, we examined the effect of TGF-β1 treatment on [^{3}H]D-glucose uptake in A549 cells. D-glucose uptake was enhanced at 6, 9, and 12 h, but not at 24 and 72 h after treatment (Supplementary Fig. 3). In addition,

GHB uptake was not affected by TGF-β1 at 24 h (data not shown). These findings suggest that, in an early phase, TGF-β1 may stimulate glucose uptake, while in a later phase, MCT1 function is upregulated for oxidative metabolism in A549 cells. However, further studies are needed to clarify the mechanisms underlying such a metabolic shift during TGF-β1-induced EMT.

In addition to organ fibrosis, EMT also contributes to cancer progression, and metabolic reprogramming in cancer cells is well characterized. Tumors frequently display a glycolytic phenotype with increased uptake of glucose for glycolysis and concomitant synthesis of lactate (Morais-Santos et al. 2015). The lactate produced by hypoxic tumor cells may diffuse and be taken up by oxygenated tumor cells (Feron 2009). MCT1 regulates the entry of lactate into oxidative tumor cells (Fiaschi et al. 2012). Therefore, higher MCT1 expression is assumed to be a prognostic indicator in human neuroblastoma and melanoma cell lines (Fang et al. 2006; Zhang et al. 2018). Moreover, Choi et al. (2014) reported that high MCT1 expression levels correlated with high tumor grade, advanced tumor stage, and lymphatic tumor invasion. Based on these studies, we examined the effect of CHC and AR on TGF-β1 induced EMT in A549 cells. Although CHC and AR clearly inhibited GHB and LA uptakes in A549 cells, CHC and AR did not affect TGF-β1-induced EMT-like morphological changes. Moreover, CHC and AR did not affect TGF-β1-induced changes in mRNA expression related to EMT, indicating that MCT1 transport function may not directly contribute to TGF-β1-induced EMT in A549 cells. Gray et al. (2016) demonstrated that knockdown of MCT1 (but not AZD3965, a promising MCT1 inhibitor) suppressed hepatocyte growth factor- and epidermal growth factor-induced tumor cell scattering and

wound healing. Thus, our results suggest that MCT1 transport activity may not be crucial to the EMT process. Therefore, factors other than the transporter activity of MCT1 may be responsible for TGF-β1-induced EMT in A549 cells.

Conversely, TGF-β1 is produced as a latent complex, and activation of TGF-β1 generally requires the binding of αv integrin to an RGD motif in the latent form of TGF-β1 (Shi et al. 2011). Alterations in pH resulting from endogenous production and release of LA is reportedly capable of activating latent TGF-β1 (Kottmann et al. 2012). In this context, LA concentration, which is regulated by MCT1, may be a key component during TGF-β1-induced EMT under *in vivo* conditions. Therefore, the relationship between MCT1 expression level, transporter activity of MCT1, and induction of EMT by TGF-β1 needs to be studied further.

9. Conclusions

We characterized MCT1 function in A549 cells and found that functional expression of MCT1 was upregulated by TGF-β1 treatment via the TGF-β1 signaling pathway, as evidenced by an inhibitory effect of SB. These findings may help in understanding the association of metabolic reprogramming with TGF-β1-induced EMT in alveolar epithelial cells.

10. Author’s contributions

MU and MK designed and performed the experiments, analyzed the data, and wrote the manuscript. RY and MT discussed the results and edited and approved the manuscript.

11. Conflict of interest statement

The authors declare that there are no conflicts of interest.

12. References

Bröer S, Bröer A, Schneider HP, et al (1999) Characterization of the high-affinity monocarboxylate transporter MCT2 in Xenopus laevis oocytes. Biochem J 341:529–35. https://doi.org/10.1042/0264-6021:3410529

Choi J-W, Kim Y, Lee J-H, Kim Y-S (2014) Prognostic significance of lactate/proton symporters MCT1, MCT4, and their chaperone CD147 expressions in urothelial carcinoma of the bladder. Urology 84:245.e9–15. https://doi.org/10.1016/j.urology.2014.03.031

Connolly EC, Freimuth J, Akhurst RJ (2012) Complexities of TGF-β targeted cancer therapy. Int J Biol Sci 8:964–78. https://doi.org/10.7150/ijbs.4564

Doherty JR, Yang C, Scott KE, et al (2014) Blocking lactate export by inhibiting the Myc target MCT1 Diables glycolysis and glutathione synthesis. Cancer Res 74:908-20. https://doi.org/10.1158/0008-5472.CAN-13-2034

Eilertsen M, Andersen S, Al-Saad S, et al (2014) Monocarboxylate transporters 1-4 in NSCLC: MCT1 is an independent prognostic marker for survival. PLoS One 9:e105038. https://doi.org/10.1371/journal.pone.0105038

Fang J, Quinones QJ, Holman TL, et al (2006) The H+-linked monocarboxylate transporter (MCT1/SLC16A1): a potential therapeutic target for high-risk neuroblastoma. Mol Pharmacol 70:2108–15. https://doi.org/10.1124/mol.106.026245

Feron O (2009) Pyruvate into lactate and back: from the Warburg effect to symbiotic energy fuel exchange in cancer cells. Radiother Oncol 92:329–33. https://doi.org/10.1016/j.radonc.2009.06.025

Fiaschi T, Marini A, Giannoni E, et al (2012) Reciprocal metabolic reprogramming through lactate shuttle coordinately influences tumor-stroma interplay. Cancer Res 72:5130–40. https://doi.org/10.1158/0008-5472.CAN-12-1949

Fishbein WN, Merezhinskaya N, Foellmer JW (2002) Relative distribution of three major lactate transporters in frozen human tissues and their localization in unfixed skeletal muscle. Muscle Nerve 26:101–112. https://doi.org/10.1002/mus.10168

Gray AL, Coleman DT, Shi R, Cardelli JA (2016) Monocarboxylate transporter 1 contributes to growth factor-induced tumor cell migration independent of transporter activity. Oncotarget 7:32695-706. https://doi.org/10.18632/oncotarget.9016

Guan X, Rodriguez-Cruz V, Morris ME (2019) Cellular uptake of MCT1 inhibitors AR-C155858 and AZD3965 and their effects on MCT-mediated transport of l-lactate in murine 4T1 breast tumor cancer cells. AAPS J 21:13. https://doi.org/10.1208/s12248-018-0279-5

Guan X, Ruszaj D, Morris ME (2018) Development and validation of a liquid chromatography tandem mass spectrometry assay for AZD3965 in mouse plasma and tumor tissue: Application to pharmacokinetic and breast tumor xenograft studies. J Pharm Biomed Anal 155:270–275. https://doi.org/10.1016/j.jpba.2018.03.061

Halestrap AP, Meredith D (2004) The SLC16 gene family-from monocarboxylate transporters (MCTs) to aromatic amino acid transporters and beyond. Pflugers Arch 447:619–28. https://doi.org/10.1007/s00424-003-1067-2

Halestrap AP, Wilson MC (2012) The monocarboxylate transporter family--role and regulation. IUBMB Life 64:109–19. https://doi.org/10.1002/iub.572

Kalluri R, Neilson EG (2003) Epithelial-mesenchymal transition and its implications for fibrosis. J Clin Invest 112:1776–84. https://doi.org/10.1172/JCI20530
Kalluri R, Weinberg RA (2009) The basics of epithelial-mesenchymal transition. J Clin Invest 119:1420–8. https://doi.org/10.1172/JCI39104
Kang H, Kim H, Lee S, et al (2019) Role of metabolic reprogramming in epithelial–mesenchymal transition (EMT). Int J Mol Sci 20:2042. https://doi.org/10.3390/ijms20082042
Kawami M, Deguchi J, Yumoto R, et al (2017) Effect of COA-Cl on transforming growth factor-β1-induced epithelial-mesenchymal transition in RLE/Abca3 cells. Drug Metab Pharmacokinet 32:224-227. https://doi.org/10.1016/j.dmpk.2017.05.001.
Kawami M, Harabayashi R, Harada R, et al (2018a) Folic acid prevents methotrexate-induced epithelial-mesenchymal transition via suppression of secreted factors from the human alveolar epithelial cell line A549. Biochem Biophys Res Commun 497:457–463. https://doi.org/10.1016/j.bbrc.2018.02.111
Kawami M, Harabayashi R, Miyamoto M, et al (2016) Methotrexate-induced epithelial–mesenchymal transition in the alveolar epithelial cell line A549. Lung 194:923–930. https://doi.org/10.1007/s00408-016-9935-7
Kawami M, Yamada Y, Issarachot O, et al (2018b) P-gp modulating effect of Azadirachta indica extract in multidrug-resistant cancer cell lines. Pharmazie 73:104–109. https://doi.org/10.1691/ph.2018.7116
Kottmann RM, Kulkarni AA, Smolnycki KA, et al (2012) Lactic acid is elevated in idiopathic pulmonary fibrosis and induces myofibroblast differentiation via pH-dependent activation of transforming growth factor-β. Am J Respir Crit Care Med 186:740–751. https://doi.org/10.1164/rccm.201201-0084OC
Lieber M, Smith B, Szakal A, et al (1976) A continuous tumor-cell line from a human lung carcinoma with properties of type II alveolar epithelial cells. Int J cancer 17:62–70
Liu M, Quek L-E, Sultani G, Turner N (2016) Epithelial-mesenchymal transition induction is associated with augmented glucose uptake and lactate production in pancreatic ductal adenocarcinoma. Cancer Metab 4:19. https://doi.org/10.1186/s40170-016-0160-x
Lottes RG, Newton DA, Spyropoulos DD, Baatz JE (2014) Alveolar type II cells maintain bioenergetic homeostasis in hypoxia through metabolic and molecular adaptation. Am J Physiol Lung Cell Mol Physiol 306:L947-55. https://doi.org/10.1152/ajplung.00298.2013
Lottes RG, Newton DA, Spyropoulos DD, Baatz JE (2015) Lactate as substrate for mitochondrial respiration in alveolar epithelial type II cells. Am J Physiol Lung Cell Mol Physiol 308:L953-61. https://doi.org/10.1152/ajplung.00335.2014
Morais-Santos F, Granja S, Miranda-Gonçalves V, et al (2015) Targeting lactate transport suppresses in vivo breast tumour growth. Oncotarget 6:19177–89. https://doi.org/10.18632/oncotarget.3910
Morandi A, Taddei ML, Chiarugi P, Giannoni E (2017) Targeting the metabolic reprogramming that controls epithelial-to-mesenchymal transition in aggressive tumors. Front Oncol 7:40. https://doi.org/10.3389/fonc.2017.00040
Payen VL, Mina E, Van Hee VF, Porporato PE, Sonveaux P (2019) Monocarboxylate

transporters in cancer. Mol Metab. https://doi.org/10.1016/j.molmet.2019.07.006
Pinheiro C, Longatto-Fiho A, Azevedo-Silva J, et al (2012) Role of monocarboxylate transporters in human cancers: state of the art. J Bioenerg Biomembr 44:127-39. https://doi.org/10.1007/s10863-012-9428-1
Shi M, Zhu J, Wang R, et al (2011) Latent TGF-β structure and activation. Nature 474:343–9. https://doi.org/10.1038/nature10152
Takano M, Yamamoto C, Yamaguchi K, et al (2015) Analysis of TGF-β1- and drug-induced epithelial-mesenchymal transition in cultured alveolar epithelial cell line RLE/Abca3. Drug Metab Pharmacokint 30:111-8. https://doi.org/10.1016/j.dmpk.2014.10.007
Tuder RM, Lara AR, Thannickal VJ (2012) Lactate, a novel trigger of transforming growth factor-β activation in idiopathic pulmonary fibrosis. Am J Respir Crit Care Med 186:701–3. https://doi.org/10.1164/rccm.201208-1491ED
Ullah MS, Davies AJ, Halestrap AP (2006) The plasma membrane lactate transporter MCT4, but not MCT1, is up-regulated by hypoxia through a HIF-1alpha-dependent mechanism. J Biol Chem 281:9030–7. https://doi.org/10.1074/jbc.M511397200
Willis BC, Borok Z (2007) TGF-β-induced EMT: mechanisms and implications for fibrotic lung disease. Am J Physiol Lung Cell Mol Physiol 293:L535-34. https://doi.org/10.1152/ajplung.00163.2007
Xie N, Tan Z, Banerjee S, et al (2015) Glycolytic reprogramming in myofibroblast differentiation and lung fibrosis. Am J Respir Crit Care Med 192:1462–1474. https://doi.org/10.1164/rccm.201504-0780OC
Zank DC, Bueno M, Mora AL, Rojas M (2018) Idiopathic pulmonary fibrosis: aging, mitochondrial dysfunction, and cellular bioenergetics. Front Med 5:10. https://doi.org/10.3389/fmed.2018.00010
Zhang G, Zhang Y, Dong D, et al (2018) MCT1 regulates aggressive and metabolic phenotypes in bladder cancer. J Cancer 9:2492–2501. https://doi.org/10.7150/jca.25257

13. Figure captions

Fig. 1 (a) Time- and temperature-dependence of [^{3}H]GHB and [^{3}H]LA uptake in A549 cells. The cells were incubated with [^{3}H]GHB (100 nM) and [^{3}H]LA (1 mM) for 0.25, 0.5, 1, 3, and 5 min at 37 °C (open circles) or 4 °C (solid circles). (b) Effect of pH on the uptake of GHB and LA in A549 cells. The cells were incubated with [^{3}H] GHB (100 nM) for 1 min at pH 7.4 (open column) or pH 6.0 (solid column). Each value represents the mean ± S.E.M. of three monolayers. **$p<0.01$, significantly different from the control.

Fig. 2 (a) Dixon plot analysis of the inhibitory effects of CHC on MCT1-mediated transport. A549 cells were incubated with [^{3}H]GHB (25 nM or 50 nM) and [^{3}H]LA (1 mM or 2 mM) for 1 min in the absence or presence of varying concentrations of CHC (0.5, 1, 2 mM) at pH 6.0. (b, c) Effect of phloretin and LA on the uptake of GHB in A549 cells. The cells were incubated with [^{3}H]GHB (50 nM) for 1 min in the absence or presence of various concentrations of phloretin (10, 20, 100 μM) or LA (1, 5, 10 mM) at pH 6.0. (d) Effect of AR on the uptakes of GHB and LA in A549 cells. The cells were incubated with [^{3}H]GHB (50 nM) or [^{3}H]LA (1 mM) for 1 min in the absence or presence of various concentrations of AR (1, 3, 6, 10, 30, 100, 1000 μM) at pH 6.0. Each value represents the mean ± S.E.M. of three monolayers. **$p<0.01$, significantly different from the control.

Fig. 3 Role of the TGF-β1 signaling cascade pathway on the function (a) and mRNA/protein expression levels (b, c) of MCT1 in A549 cells. The cells were treated with TGF-β1 (10 ng/mL) for 72 h in the absence or presence of SB (10 μM). After that, the treated cells were incubated with [^{3}H]GHB (100 nM) and [^{3}H]LA (1 mM) in the absence or presence of CHC (2 mM). GHB uptake value was calculated by subtracting [^{3}H]GHB and [^{3}H]LA amounts with CHC from that without CHC. mRNA and protein expression levels were evaluated by real-time PCR and western blot using total RNA and crude membrane fraction extracted from the treated cells, respectively. Each value represents the mean ± S.E.M. of three monolayers. *$p< 0.05$, **$p< 0.01$, significantly different from control cells. $^{\dagger}p< 0.05$, $^{\dagger\dagger}p< 0.01$, significantly different from TGF-β1 treated cells.

Fig. 4 Effect of CHC and AR on TGF-β1-induced changes in morphology and mRNA expression levels of CK19 and α-SMA in A549 cells. The cells were treated with TGF-β1 (10 ng/mL) in the absence or presence of CHC (2 mM) or AR (1000 nM) for 72 h. After that, the morphology was observed by phase-contrast microscopy (a), and the mRNA expression levels of CK19 and α-SMA after co-treatment with CHC (b) or AR (c) were analyzed by real-time PCR using total RNA extracted from the treated cells. Each value represents the mean ± S.E.M. of three monolayers. *$p< 0.05$, **$p< 0.01$, significantly different from control cells.

Fig. 1.

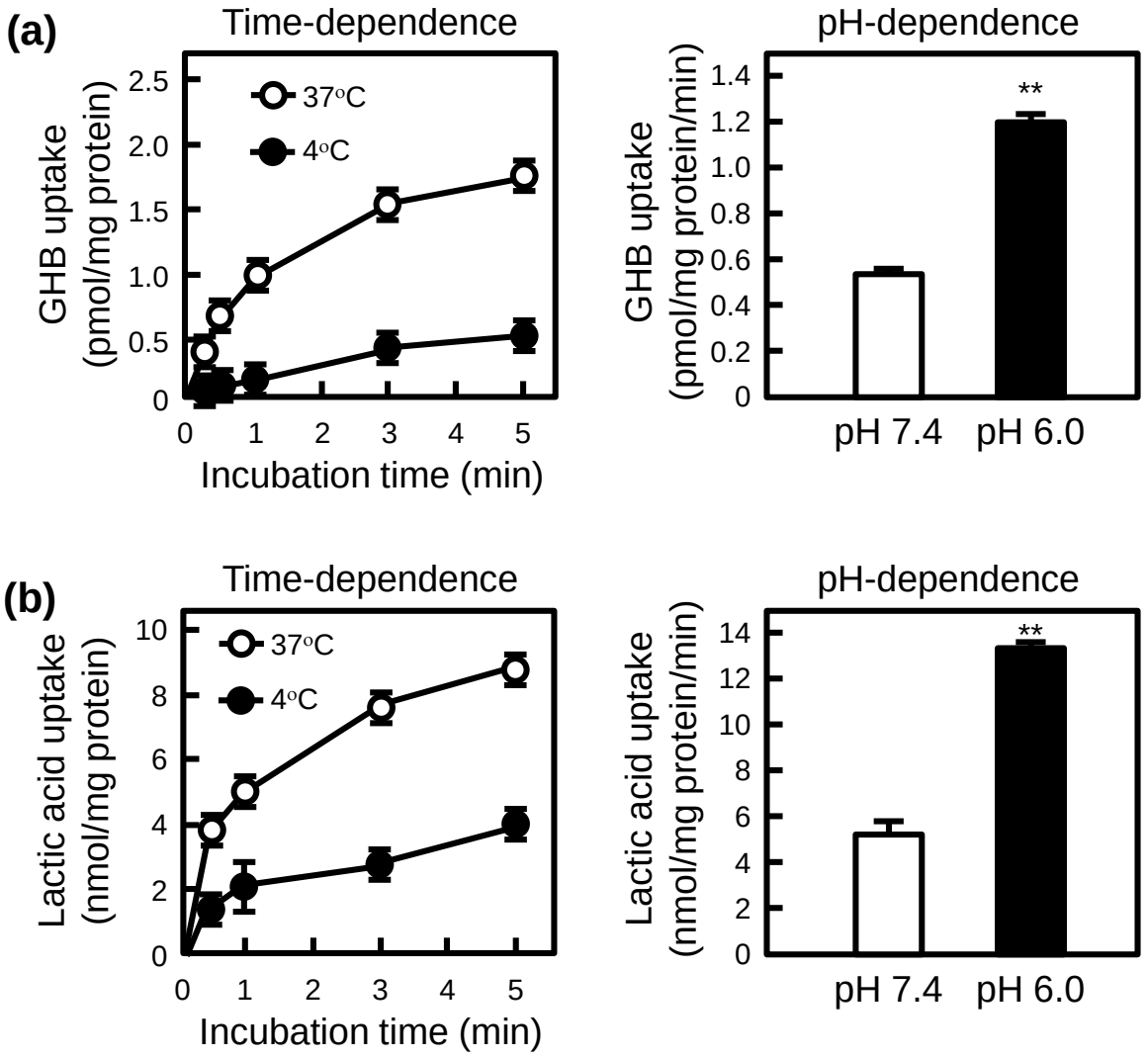
(a)
Time-dependence
GHB uptake (pmol/mg protein)
37°C
4°C
Incubation time (min)
pH-dependence
GHB uptake (pmol/mg protein/min)
**
pH 7.4
pH 6.0
(b)
Time-dependence
Lactic acid uptake (nmol/mg protein)
37°C
4°C
Incubation time (min)
pH-dependence
Lactic acid uptake (nmol/mg protein/min)
**
pH 7.4
pH 6.0

Fig. 2.

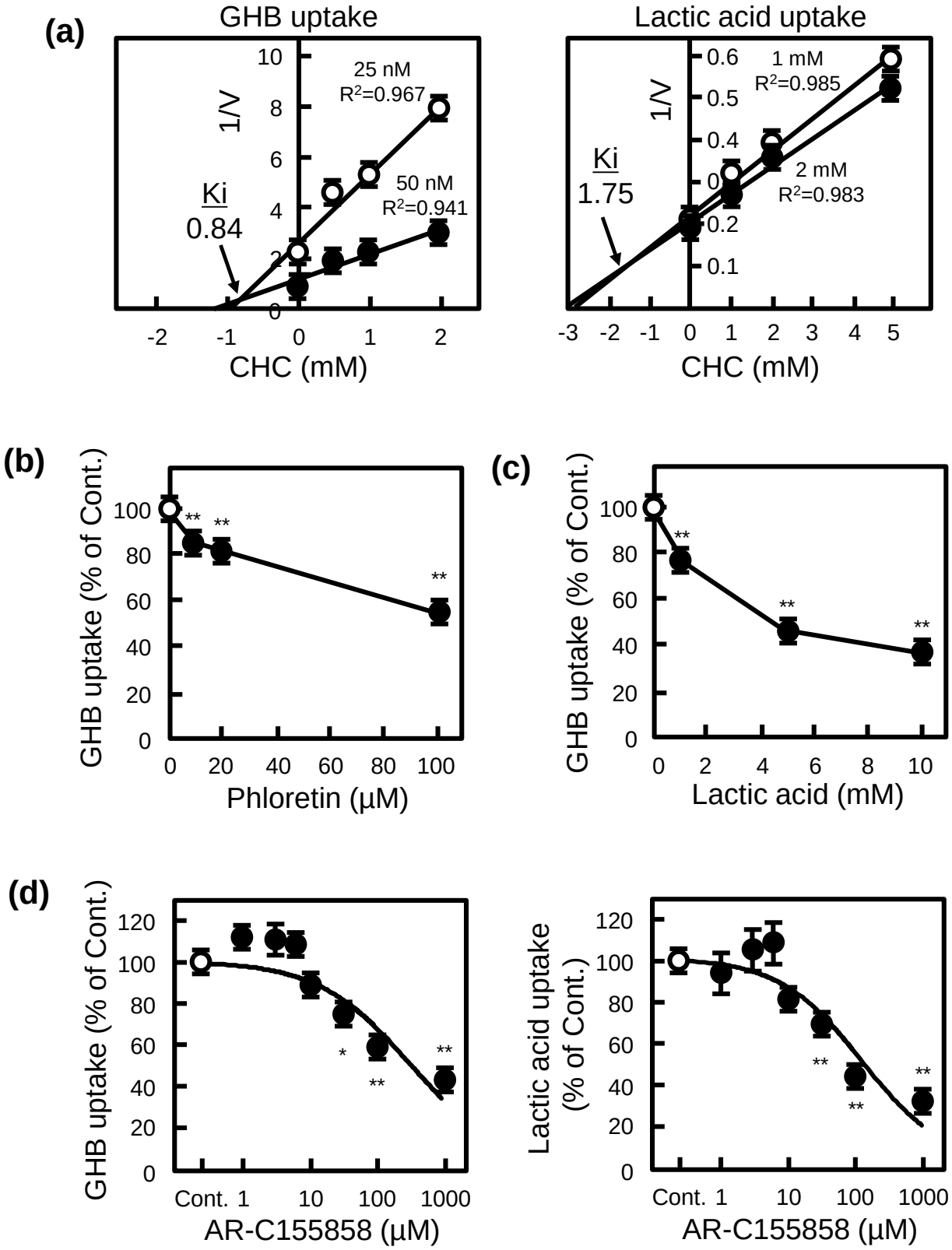
(a)
GHB uptake
1/V
25 nM
R2=0.967
50 nM
R2=0.941
Ki
0.84
CHC (mM)
Lactic acid uptake
1 mM
R2=0.985
2 mM
R2=0.983
Ki
1.75
CHC (mM)
(b)
GHB uptake (% of Cont.)
Phloretin (μM)
(c)
GHB uptake (% of Cont.)
Lactic acid (mM)
(d)
GHB uptake (% of Cont.)
Cont. 1 10 100 1000
AR-C155858 (μM)
Lactic acid uptake (% of Cont.)
Cont. 1 10 100 1000
AR-C155858 (μM)

Fig. 3.

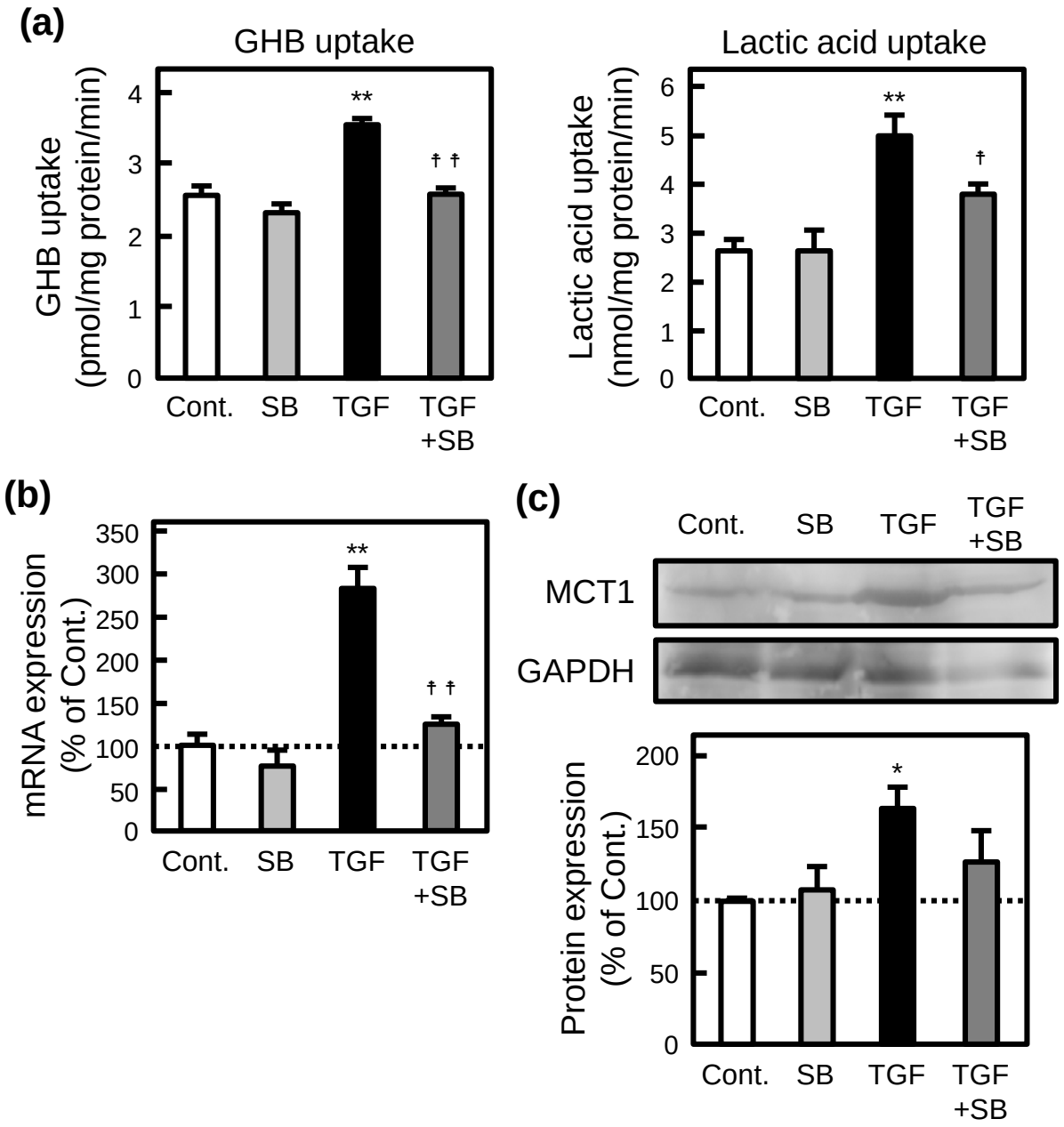
(a)
GHB uptake
GHB uptake (pmol/mg protein/min)
0
1
2
3
4
**
† †
Cont.
SB
TGF
TGF +SB
Lactic acid uptake
Lactic acid uptake (nmol/mg protein/min)
0
1
2
3
4
5
6
**
†
Cont.
SB
TGF
TGF +SB
(b)
mRNA expression (% of Cont.)
0
50
100
150
200
250
300
350
**
† †
Cont.
SB
TGF
TGF +SB
(c)
Cont.
SB
TGF
TGF +SB
MCT1
GAPDH
Protein expression (% of Cont.)
0
50
100
150
200
*
Cont.
SB
TGF
TGF +SB

Fig. 4.

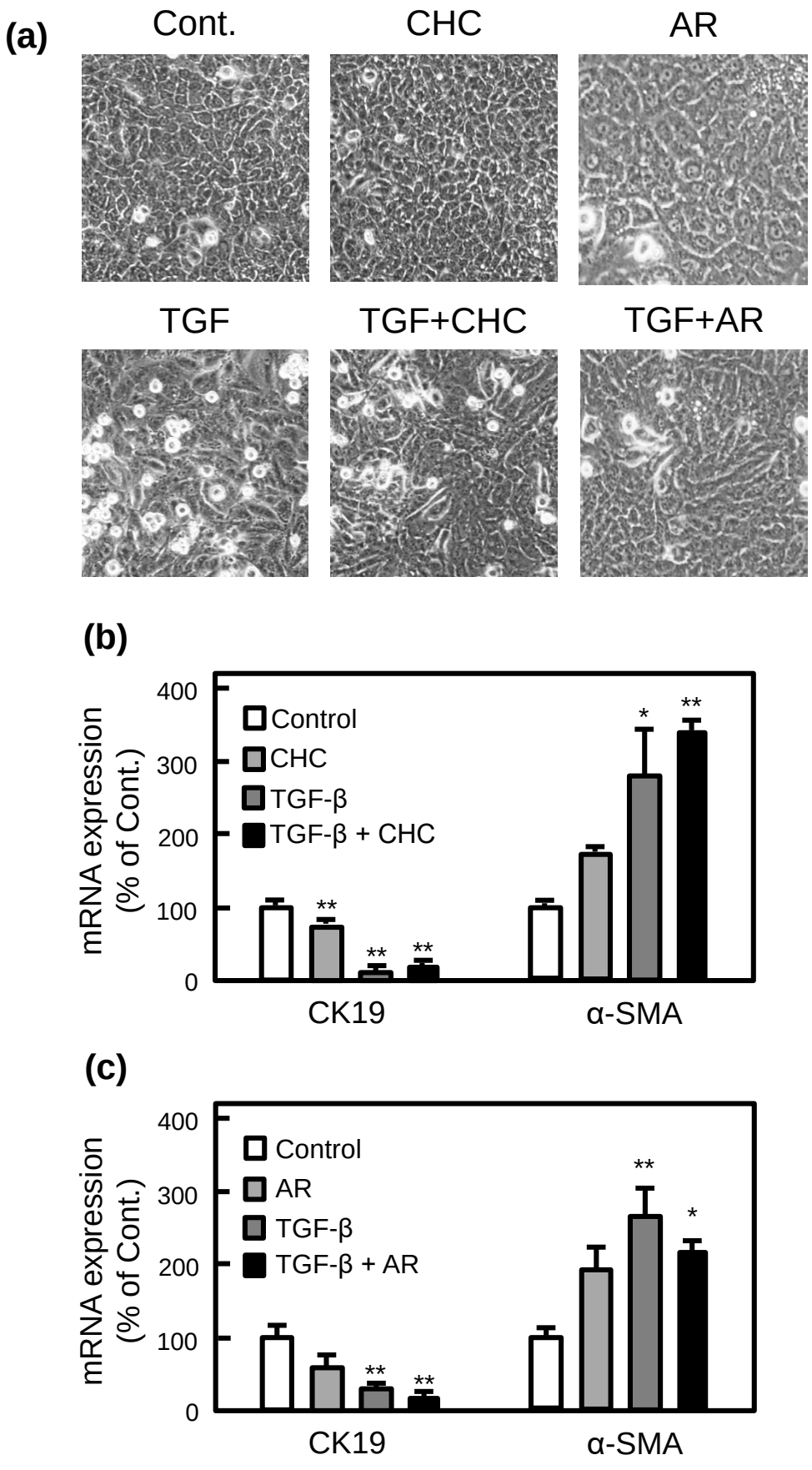
(a)
Cont.
CHC
AR
TGF
TGF+CHC
TGF+AR
(b)
mRNA expression (% of Cont.)
400
300
200
100
0
Control
CHC
TGF-β
TGF-β + CHC
**
**
**
*
**
CK19
α-SMA
(c)
mRNA expression (% of Cont.)
400
300
200
100
0
Control
AR
TGF-β
TGF-β + AR
**
**
**
*
CK19
α-SMA

Supplementary Fig. 1

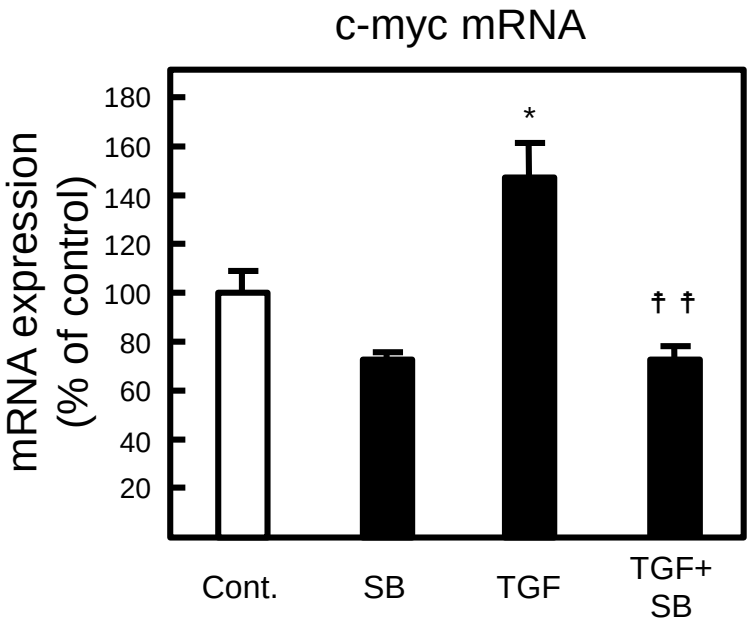

Supplementary Fig. 1. Effect of TGF-β1 signaling pathway on mRNA expression level of c-myc in A549 cells. The cells were treated with TGF-β1 (10 ng/mL) in the absence or presence of SB (10 μM) for 72 h. The mRNA expression level of c-myc was analyzed by real-time PCR as described in the Materials and Methods section. Each value represents the mean ± S.E.M. of three monolayers. **p<0.01, significantly different from control. † †p<0.01, significantly different from control.

Supplementary Fig. 2

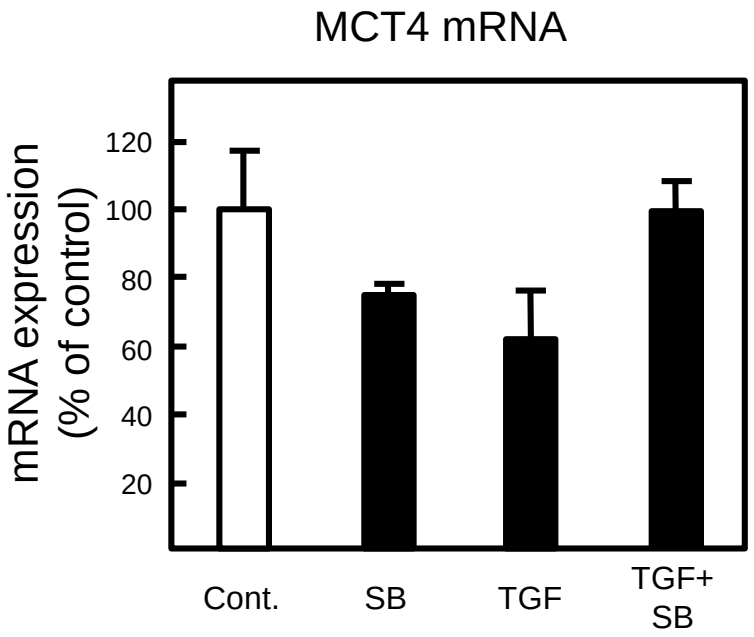

Supplementary Fig. 2. Effect of TGF-β1 signaling pathway on the mRNA expression level of MCT4 in A549 cells. The cells were treated with TGF-β1 (10 ng/mL) in the absence or presence of SB (10 μM) for 72 h. mRNA expression level of MCT4 was analyzed by real-time PCR as described in the Materials and Methods section. Each value represents the mean ± S.E.M. of three monolayers.

Supplementary Fig. 3

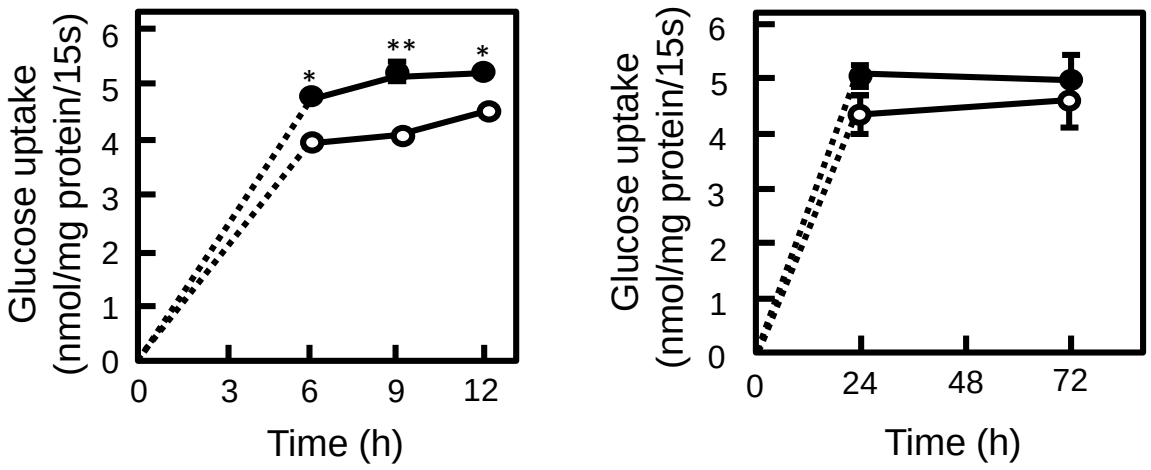

Supplementary Fig. 3. Effect of TGF-β1 treatment at different time intervals on GLUT1 function in A549 cells. The cells were not pretreated (open circle) or were pretreated with TGF-β1 (solid circle) for 6, 9, and 12 h (a), or 24 and 72 h (b), respectively. The glucose uptake experiment was performed using [^{3}H]D-Glucose as a substrate. Each value represents the mean ± S.E.M. of three monolayers. *p<0.05, **p<0.01, significantly different from control.